

## TRANSFORMATION AND CALIBRATION OF PICTURES IN THE FOTOM SYSTEM

Lačezar Ličev<sup>1</sup>, Jan Král<sup>2</sup>

<sup>1</sup>Department of Computer Science, FEECS, VŠB - Technical University of Ostrava  
708 33, Ostrava, Czech republic  
*Contact: lacezar.licev@vsb.cz*

<sup>2</sup>Department of Computer Science, FEECS, VŠB - Technical University of Ostrava  
708 33, Ostrava, Czech republic  
*Contact: jn.kral@gmail.com*

### Abstract.

The FOTOM system developed at the Department of Computer Science FEECS VŠB TU Ostrava is used for digital image processing. FOTOM 2008 was created in the programming language C++. In 2009, a new, revolutionary version of the system, FOTOM 2009, was designed. This new system has new kernel and provides a more universal and easily extensible architecture with newly solved calibration and transformation images.

Mine image transformations consist of conversion data from snapshots to the three - dimensional coordinate system. Calibration images and acquired variables are used for corrective projection allowing for easier measuring of observed objects. Calibration images also support the transformation of objects recumbent on the inner wall of a cylindrical object.

**Keywords:** architecture, photogrammetry, FOTOM 2000, 2008, 2009, Java, calibration, Netbeans platform, projection, transformation, xml, interest object, image processing.

## 1 INTRODUCTION

This report addresses modern methods used for processing images and, in particular, measuring the objects present in them. Using the program / module for calibration and transformation of images within the framework of FOTOM 2008 and 2009 systems, a new generation of the FOTOM system has been created.

Data is converted from snapshots to 3D coordinate systems during the transformation of mine images. When calibrating images, we acquire variables that are useful in corrective projection and allow us to measure observed objects more easily. Calibrating images also aids in the transformation of objects recumbent on the inner wall of a cylindrical object. These images can be used to measure objects found on inner wall of a mine - 2D image.

## 2 IMAGING METHODS AND MINE MEASURING

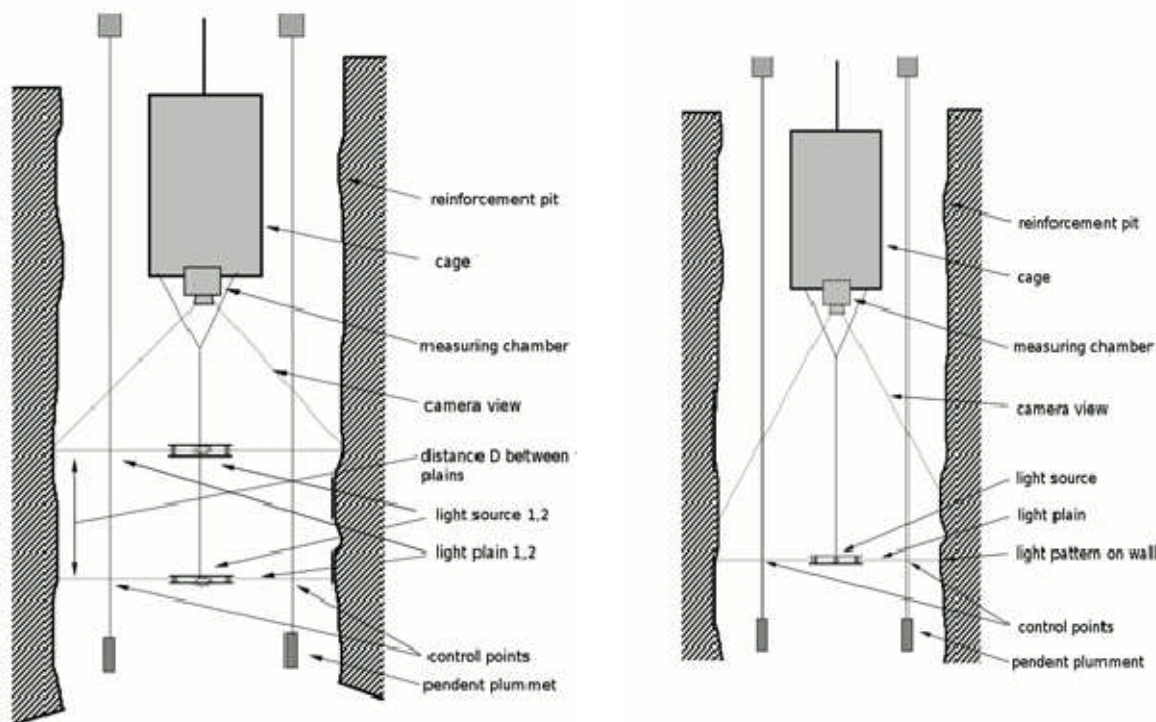
### 2.1 Measuring methods used at VVUÚ Ostrava-Radvanice and BMZ VŠB TUO

The method used in diagnosing pits [1-3, 6] presents a single-image photogrammetric method making use of two luminary plains at the same time, see picture 2.1. In both images, there are two horizontal profiles displayed with a common constant vertical distance  $D$ . This principle rests upon the fact that in the original profile we regulate the photogrammetric set so that the higher of the two luminary plains is at the exact same level as the initial profile. We then select at least two appropriate points in the profile whose mutual position we determine. Following exposure, not only will the initial image be displayed, but the following image will be displayed as well. Once the entire set is activated with value  $D$ , the upper luminary plain level will be at the level of profile No. 2, and profile No. 3 will be decreased by the value of  $D$ . This process is repeated through all depths of the pit being measured.

The method used at BMZ VŠB TUO [5, 7], which was implemented to diagnose pits, presents a single-image photogrammetric method using one luminary plain (see picture No. 2.1.) In each image, not only are the given profile pits, guide, and pipeline captured, but the intersection luminary plains with wire plumb lines are

captured as well. The distances of the photo-chambers and plain are constant, therefore the scale of all images is the same.

Prior to measuring, it is necessary to select an acceptable interval of survey profiles (etc. 10 m) and mark their position in the pit. The disadvantage in using this method lies in the difficulty of manipulating when using plumb lines, resulting in the necessity for longer pauses in movement within the pit. At larger depths, a laborious stabilization or rehangng of plumb lines is necessary.



VVUÚ Ostrava-Radvanice

BMZ VŠB TU Ostrava.

**Fig. 2.1.** Photogrammetric kit.

Imaging is processed with the aid of the photogrammetric kit developed by BMZ VŠB TU Ostrava and VVUÚ Ostrava-Radvanice. The kit (see picture No. 2.1) is pieced together by a surveying camera (aerial photogrammetry chamber AFP 21 Soviet production format 13x18 cm.), which is hung below the cage. Below the camera is hung the upper light source is hung 6m below the camera ( $D = 6m$ ). This is special flash equipment equipped with an orbicular lens that generates a luminous plain (designed at the former Ore Research Institute of Prague). When measuring, a control panel is placed inside the container, upon which a metal sheet cover attached is placed simultaneously attached to a 24V accumulator battery. This control panel ensures the entire process. The total length of the device below the cage is about 18m.

A 1m measuring wheel is placed in the engine room to measure the distance traveled.

## 2.2 Transformation of mine images in the FOTOM system

The method used to analyze mine images [7, 8, 10-14] belongs to the single-image photogrammetry category. This means that we can only determine 2D coordinates in the plain of the photographed object based on the position of the photo-station and orientation of the photographed object plain. In our case, this subject is the above-mentioned light plain which leaves a light-footprint on the profile pits and other devices. If we observe only the lit places (points), belonging to the light-footprint, we can clearly identify their position in the global coordinate system.

Now we need to determine transformation relations, which will transfer data from a local (snapshot) coordinate system to a global coordinate system. These transformations belong to the category of planar affine transformations. If images are produced as described, the following conditions are met:

- luminary plain and projection plain are parallel
- the image axis is perpendicular to the plain
- distortion in the special camera lens is insignificant

$$\text{turn:} \quad \mathbf{R} = \begin{pmatrix} r_x & r_y & 0 \\ -r_y & r_x & 0 \\ 0 & 0 & 1 \end{pmatrix} \quad (2.1)$$

$$\text{shift:} \quad \mathbf{T} = \begin{pmatrix} 1 & 0 & 0 \\ 0 & 1 & 0 \\ t_x & t_y & 1 \end{pmatrix} \quad (2.2)$$

$$\text{scaling:} \quad \mathbf{S} = \begin{pmatrix} 1 & 0 & 0 \\ 0 & 1 & 0 \\ 0 & 0 & \frac{1}{s} \end{pmatrix} \quad (2.3)$$

The transformation point is then expressed by the matrix equation

$$\mathbf{X}' = \mathbf{X} \cdot \mathbf{Tr} \quad (2.4)$$

where  $X'$  is the row vector representing the position of the transformed point after the transformation,  $X$  is a row vector representing the position of the transition point and  $Tr$  is the transformation matrix.

Then the overall transformation matrix is represented as:

$$\mathbf{Tr} = \mathbf{R} \cdot \mathbf{S} \cdot \mathbf{T} = \begin{pmatrix} r_x & r_y & 0 \\ -r_y & r_x & 0 \\ 0 & 0 & 1 \end{pmatrix} \cdot \begin{pmatrix} 1 & 0 & 0 \\ 0 & 1 & 0 \\ 0 & 0 & \frac{1}{s} \end{pmatrix} \cdot \begin{pmatrix} 1 & 0 & 0 \\ 0 & 1 & 0 \\ t_x & t_y & 1 \end{pmatrix} = \begin{pmatrix} r_x & r_y & 0 \\ -r_y & r_x & 0 \\ \frac{t_x}{s} & \frac{t_y}{s} & \frac{1}{s} \end{pmatrix}$$

(2.5)

We now need to determine the coefficients  $r_x$ ,  $r_y$ ,  $t_x$ ,  $t_y$  a  $s$ . Let us set an auxiliary function of the two variables **atg2**, from which the parameters  $x$  and  $y$  calculate the deflection line angle of points  $[0, 0]$  and  $[x, y]$  from the positive half  $x$ -axis. It is now a function with field values  $(-p, p)$ .

The transformation is derived from the knowledge of the two pairs of corresponding control points. Local control points are designate as  $L1$  and  $L2$ , corresponding to the global control points  $G1$  and  $G2$ . Further, let us introduce  $\Delta L$  as the distance between points  $L1$  and  $L2$ :

$$\Delta L = \sqrt{(L2_x - L1_x)^2 + (L2_y - L1_y)^2} \quad (2.6)$$

Likewise,  $\Delta G$  is the distance between points G1 and G2. The angle rotation is designated as  $\psi$ :

$$\psi = \text{atg}2(G2_y - G1_y, G2_x - G1_x) - \text{atg}2(L2_y - L1_y, L2_x - L1_x) \quad (2.7)$$

Then the transformation coefficients are:

$$s = \frac{\Delta G}{\Delta L} \quad (2.8)$$

$$r_x = \cos(\psi) \quad (2.9)$$

$$r_y = \sin(\psi) \quad (2.10)$$

$$t_x = G1_x - s \cdot (L1_x r_x - L1_y r_y) \quad (2.11)$$

$$t_y = G1_y - s \cdot (L1_y r_x + L1_x r_y) \quad (2.12)$$

### Factors affecting measurement accuracy

This issue is relatively vast, therefore, we shall limit our enumeration to single factors. The most important factor affecting the accuracy of measurement (Ličev, Holusa, 1998), is to set a plumb line for the exact location of control points. Any major error can also cause a deflection of luminary plains from projection plains. Ideally, both of these plains should be horizontal. Other factors affecting accuracy include the cameras themselves (photo laboratory, lens distortion, ...) and the use of photographic materials (film, glass plates, ...). Other errors may occur when determining the coordinate points on an image (resolution of the equipment – digitizer, scanner, monitor, ...).

In conclusion, photogrammetric accuracy for measurement of vertical mine workings is primarily dependent on the quality of facilities, the photography itself and the setting positions of points on the images.

## 3 CALIBRATION AND TRANSFORMATION OF IMAGES IN THE FOTOM SYSTEM

### 3.1 FOTOM 2008

The Department of Computer Science FEECS VŠB TU Ostrava has been developing the FOTOM system for use in computer processing of digital image since 1998. At first, the system was designed to measure mine pits, but over time it has expanded into a powerful system with many modules offering advanced detection and visualization of objects of interest measurements. The architecture of this development branch carries the name FOTOM 2008 and consists of modules [15, 17-19]:

**Calibration** is a set of operations, which under specific conditions determine the relationship between value quantities that are indicated by a measuring system or a measuring instrument.

**Rotation** - Rotation templates run in virtual 3D space and correspond to rotations on the main axis object. The location calibration pattern is set using the center template, or by clicking on the image.

**Camera** – The camera can be moved in virtual space (X,Y,Z camera coordinates); the rotation of the camera is fixed in the program. The size of the resulting picture may be adjusted using the zoom function.

#### Screening:

**Perspective projection** – projection rays are derived from a single point. Perspective projection respects the optical model, which reflects what we see in the real world. At increasing distances from the observer, we model proportional changes in the objects we see, which provides a good 3D perception of a plain of projection.

**The central projection** is a special case where projection rays converge in a concentric circle in the center of an image

This projection is described by the following parameters:

- $\mathbf{a}_{x,y,z}$  – point in 3D space scene
- $\mathbf{c}_{x,y,z}$  – camera location
- $\theta_{x,y,z}$  – camera rotation (for  $\mathbf{c}_{x,y,z} = \langle 0,0,0 \rangle$  a  $\theta_{x,y,z} = \langle 0,0,0 \rangle$ , a 3D vector  $\langle 1,2,0 \rangle$  displayed in a 2D vector  $\langle 1,2 \rangle$ )
- $\mathbf{e}_{x,y,z}$  – placement of an observer in the camera space
- $\mathbf{b}_{x,y}$  – 2D projection of point  $\mathbf{a}$

First we define the point  $\mathbf{d}_{x,y,z}$  as the point of translation  $\mathbf{a}$  to the coordinate system defined by  $\mathbf{c}$ .

This is achieved by subtracting  $\mathbf{c}$  from  $\mathbf{a}$  and then applying the result of the rotation matrix  $\theta$ .

$$\begin{bmatrix} d_x \\ d_y \\ d_z \end{bmatrix} = \begin{bmatrix} 1 & 0 & 0 \\ 0 & \cos - \theta_x & \sin - \theta_x \\ 0 & -\sin - \theta_x & \cos - \theta_x \end{bmatrix} \begin{bmatrix} \cos - \theta_y & 0 & -\sin - \theta_y \\ 0 & 1 & 0 \\ \sin - \theta_y & 0 & \cos - \theta_y \end{bmatrix} \begin{bmatrix} \cos - \theta_z & \sin - \theta_z & 0 \\ -\sin - \theta_z & \cos - \theta_z & 0 \\ 0 & 0 & 1 \end{bmatrix} \left( \begin{bmatrix} a_x \\ a_y \\ a_z \end{bmatrix} - \begin{bmatrix} c_x \\ c_y \\ c_z \end{bmatrix} \right) \quad (3.1)$$

Upon breaking down the values we obtain  $d_x$ ,  $d_y$ ,  $d_z$ .

A thusly transformed point may be *projected* as a 2D plain implementing the following conversion:

$$\begin{bmatrix} f_x \\ f_y \\ f_z \\ f\omega \end{bmatrix} = \begin{bmatrix} 1 & 0 & 0 & -e_x \\ 0 & 1 & 0 & -e_y \\ 0 & 0 & 1 & 0 \\ 0 & 0 & 1/-e_z & 0 \end{bmatrix} \begin{bmatrix} d_x \\ d_y \\ d_z \\ 1 \end{bmatrix} \quad (3.2)$$

$$\begin{aligned} b_x &= f_x / f\omega \\ b_y &= f_y / f\omega \end{aligned} \quad (3.3)$$

after the transcript:

$$\begin{aligned} b_x &= (d_x - e_x)(e_z / dz) \\ b_y &= (d_y - e_y)(e_z / dz) \end{aligned} \quad (3.4)$$

where  $\mathbf{e}_z$  is the distance of the plain camera from the observer corresponding to the angle sight  $\alpha$

$$\alpha = 2 \cdot \tan^{-1}(1/e_z) \quad (3.5)$$

The resulting projection to the computer-generated image is performed with a linear interpolation of the image size.

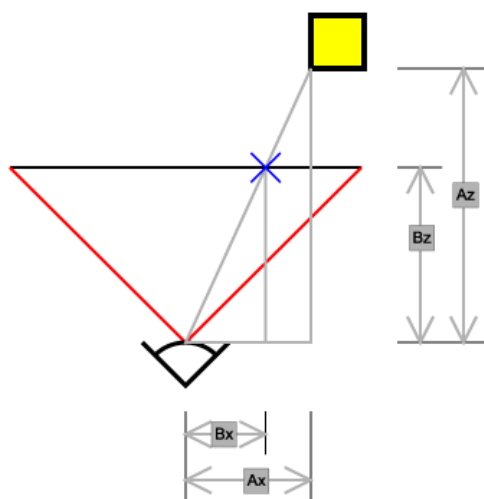


Fig. 3.1: 2D projection point.

**Transformation image:**

A calculation of the circles displayed in Figure No. 3.2 is follows. We have a total of 3 blue circles:

- $k_0$  with radius  $r_0$  = first circles, which is entered and is closest to the center
- $k_1$  with radius  $r_1$  = the largest circle in the Figure. It is presented as the second circle at the program start and should intersect with the determined starting point on the measuring axis.
- $k_2$  with radius  $r_2$  = the second largest circle in figure. This circle defines the size of first interval on the measurement axis in the pixel.

Based on these factors, the following is true:

$$r_1 - r_2 = \text{size of the first unit of scale in pixels} = U_1 \tag{3.6}$$

As for the yellow circles displayed in the Figure, the following is true :

First, the largest yellow circle is  $K_3$  with a radius  $R_3$ . This circle marks a second unit for the measuring axis.

$$r_2 - r_3 = \text{size of the second unit pixel scale} = U_2 \tag{3.7}$$

Then the ratio

$$U_2/U_1 = \Delta U = \text{the coefficient for reducing circles.} \tag{3.8}$$

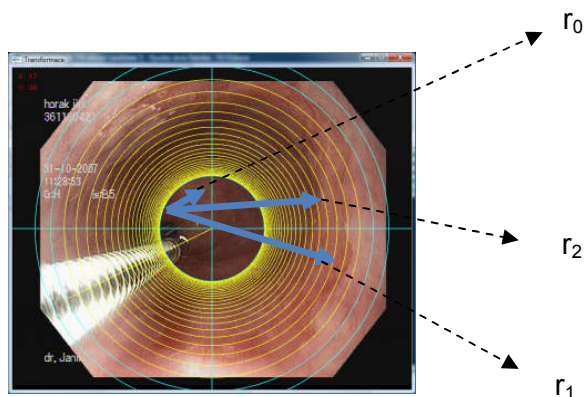


Fig. 3.2. Circle in image.

For the ensuing the yellow circles and their radius direction from circle  $k_3$  to the center, the following is true:

$$r_4 = r_3 - U_3, \quad \text{where: } U_3 = U_2 * \Delta U \tag{3.9}$$

$$r_5 = r_4 - U_4, \quad \text{where: } U_4 = U_3 * \Delta U$$

$$r_6 = r_5 - U_5, \quad \text{where: } U_5 = U_4 * \Delta U$$

etc.

In other words, a calculation for the size of ensuing units for

$$\text{measurement} = U_i = U_{i-1} * \Delta U \tag{3.10}$$

Then the radius is given by

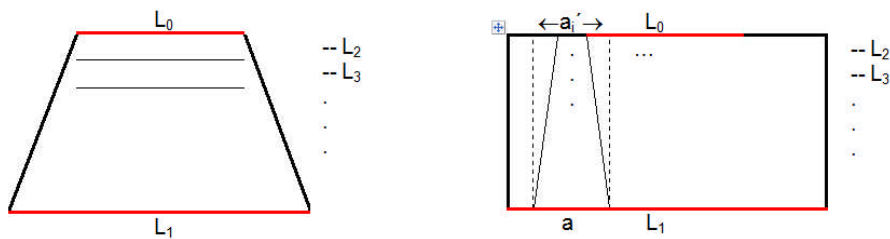
$$r_i = r_{i-1} - U_{i-1} \tag{3.11}$$

From the calculation above, we can perform the calculation of the perimeter of such circles, according to the equation:

$$L_i = 2r_i\pi \tag{3.12}$$

**Scale**

The size of the first unit is taken as the base. The unpacked image is read as a block of rows corresponding to the thickness of the units. Then, these unpacked rows transform into the first unit width. The principle of unpacking is presented below in Figure No. 3.3.



3.3a

3.3b

**Fig. 3.3.** Principle of unpacking an image.

Figure No. 3.3a is shows the shape of the unpacked image before the expansion and in Figure No. 3.3b the shape of the unpacked image after expansion is displayed. The actual expansion is performed on the basis of the calculated values of **a** and **a<sub>i</sub>'** in equation:

$$a_i' = L_i/n \tag{3.13}$$

$$a = L_1/n \tag{3.14}$$

where: **a, a<sub>i</sub>'** – the wide segments of **L<sub>1</sub>** and **L<sub>i</sub>**,

**n** – the amount of sections extended.

The logic in this exercise exists within the extending the width of section **a<sub>i</sub>'** to that of width **a**.

The result of unpacking and extending the image from Figure No. 3.2 is shown in figure No. 3.4.

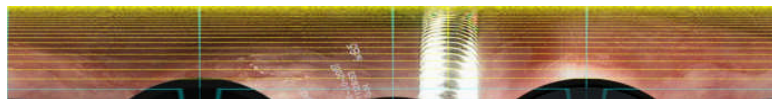


**Fig. 3.4.** Unpacking an image.

In Figure No. 3.5, a transformed image is displayed (see Figure No. 3.2), except that in addition to unpacking and extending, it is also extended in length. This extension is performed by multiplying by the constant distance between each circle. Calibration of the length of the image is also performed using this last step.

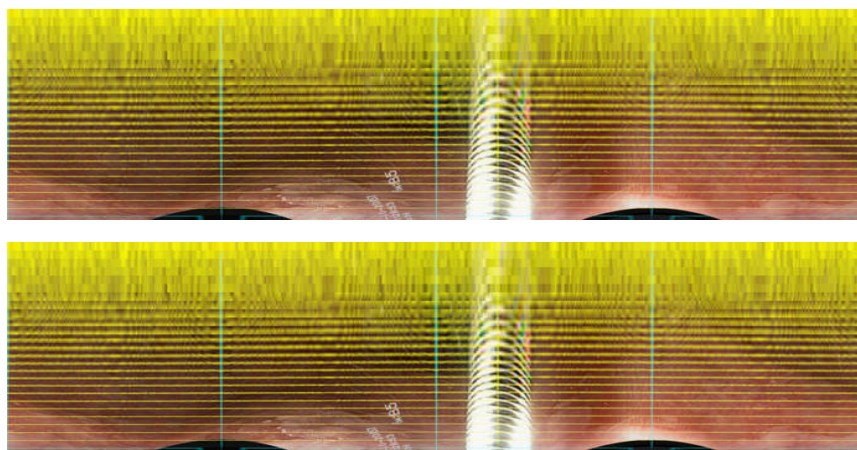


**Fig. 3.5.** Transforming the image.

The program for calibration and image transformation began with module Fotom1 of the FOTOM 2008 system. Using this program, we may project the image back onto the plain based on user-defined, design projection parameters. It is assumed that the input files are displayed using a projective view – perspective.

#### Using the program for calibration and image transformation

- Evaluation using image calibration and FOTOM 2008, without using a calibration image.
  - a. Evaluation of the object as a whole
  - b. Evaluation of the object by dividing the object into segments
  - c. Evaluation of the object using the standard
- Evaluation of an object by using calibration software and FOTOM 2008.
  - a. Using a grid-type board calibration program (see Figure No. 3.6)

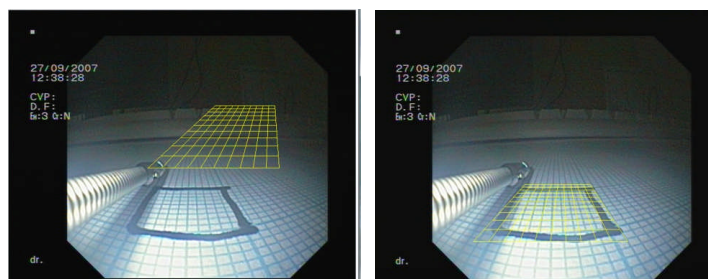


**Fig. 3.6**

- b. The use of a grid-type circle calibration program.

Using a suitable grid to localize the beginning and end of the area/region of interest.

- Evaluation using the transformation system and FOTOM 2008.

Image editing for evaluations is performed by using the calibration program. To achieve the necessary repetitious accuracy, it is necessary to determine the exact center of the image/object upon which the object is analyzed. The center can be determined in several ways, as follows:

- a. Using the transformation module calibration program
- b. Ingestion of FOTOM 2008 and a specific Fotom1 module. Here, using tools to analyze objects in the image, we may define a polygon describing the middle/center of gravity of the object being analyzed., See Figures No.3.7 and No.3.8.



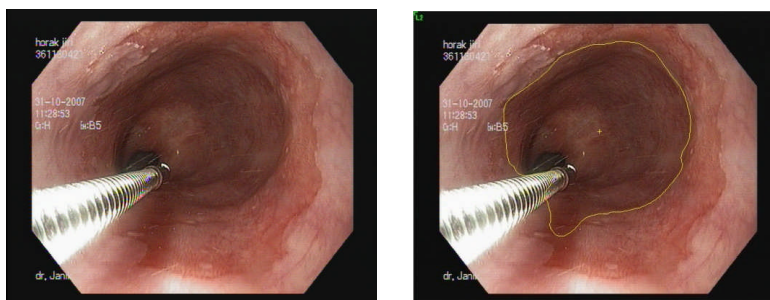


Fig. 3.7

The result of the transformation is show in Figure No. 3.8

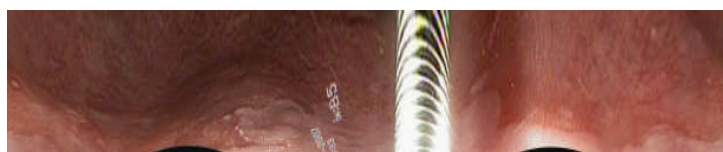


Fig. 3.8

### 3.2 System FOTOM 2009

Over the years, the development of the system FOTOM 2008 has remained a very powerful tool for digital image processing, but has gradually ceased to meet the requirements of modern applications. Originally, this system was developed as a dedicated program and did not anticipate so many developments and the extent of possible applications. The system architecture is not composed for a modular system and all resulting modules are created as a separate application and are then integrated into the system through direct intervention in the source code. Since there is no established public communication for interface modules, each module must deal with access to image processing defined objects, etc..., independantly. The consequence of these properties has resulted in an increasingly difficult expansion of the system itself, as well as individual modules.

These factors have led to the necessity to create an entirely new generation system, which would be based on a modern platform and be able to revise the system in an entirely modular way. In addition to this basic requirement, there have been other objectives introduced that have lead to the creation of a revolutionary version of FOTOM 2009 [15, 17-19].

The FOTOM 2009 application is able to export images with defined objects to the system FOTOM 2008 format, where it is possible to analyze the latest version of the system before it is implemented.

#### Calibration and transformation of images in the system FOTOM 2009

For simplification calibration is not considered with lens distortion, its processing only input digital image. However, lens distortion processing must be included for increase precision of calibration method into the future.

The output calibration is a two-dimensional image offering a parallel, right-angled, top view of an area of interest. 2D reduction results in an image proportionally showing only one level of space that is captured on the input image. The area captured in the image may contain an infinite number of plains. For successful reconstruction, the calibrated plain must be accurately defined. An integral part of this work is to program designed to calibrate a plain in space. It is necessary not only to define the plain to be calibrated, but also introduce a way to enter the plain: distance, angle plain and direction vector. This situation is illustrated in Figure No.3.9

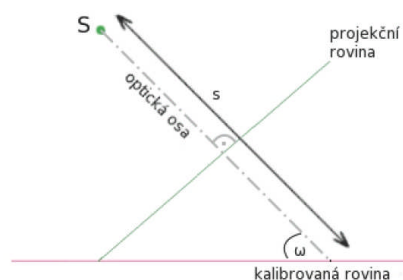


Fig. 3.9. Tilt and distance of a calibration plain.

#### Calibration process:

Calibration is focused on two kinds of images.

**Flat images** include the calibration of a general 3D image, when the calibrated surface on an image is captured as a plain. To apply this method, it is necessary to precisely define which plain captured on the image will be the object of calibration.

**The Images cavity** includes calibration of specific images created inside the hollow cylinder whose inner surface is captured on film and is the inner surface of interest intended for calibration - similar to the transformation of the image in system FOTOM 2008.

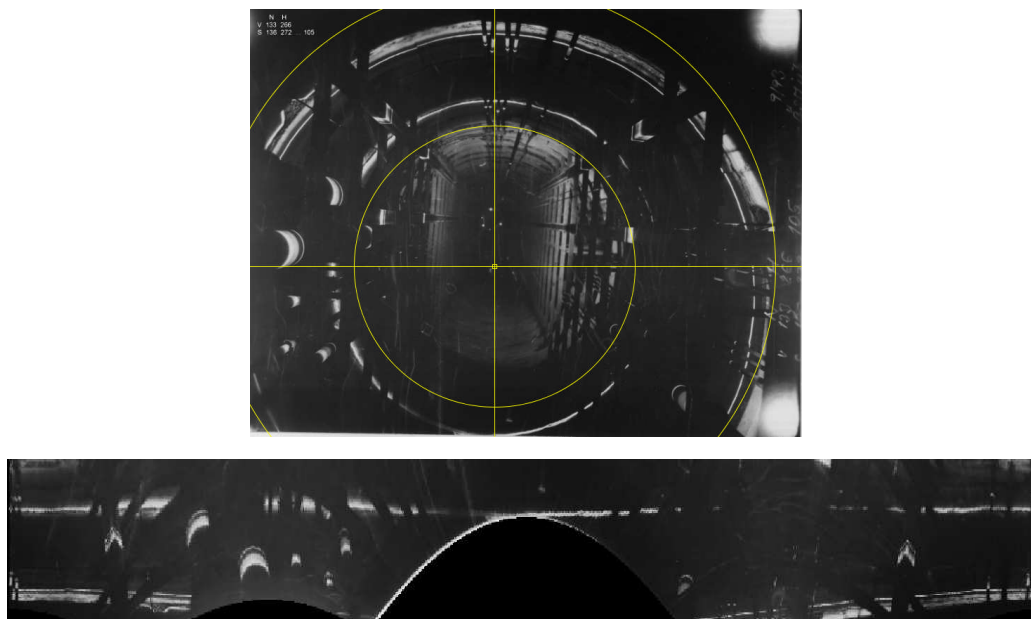


Fig. 3.10. Transformation of image mining.

## 4 RESULT

We have managed to create a new generation of FOTOM with the help of a program for calibration and transformation of images within the scope of systems FOTOM 2008 and 2009.

With mine images, transformations involve the conversion of a snapshot to a 3D coordinate system. With calibration, images acquire, among others things, variables that are used for corrective projections enabling easier measuring of observed objects. The calibration of images also supports object transformations recumbent on the inner wall of a cylindrical object. Using this, we can measure objects found on the inner wall of a mine with only a 2D image.

During the measurement process an aberration appears as a result of the lens geometric distortion. That is why the measurement accuracy of the objects of our interest is limited. The usability of implemented system is maintained through the calibration attributes preservation. This allows us to perform the same transformation

for the same part of image with similar error. The comparison of the new result with the previous one allows the user to track changes of the object size over time.

As a result is complex system that provides processing of 3D images, which can be transformed and then continue with image processing by others implemented photogrammetric functionality. System uses modern software solutions and provides simple graphic user interface. This module/program is unique and will enable us to calibrate and transform not only mining processes. Collaboration with doctors found usage of possibility to measure an object of interest in medicine.

## Reference

- [ 1] AO 175 220 o názvu "Způsob fotogrammetrického zaměřování"
- [ 2] AO 235 342 o názvu "Nosné zařízení vertikální fotogrammetrické soupravy pro měření jam z těžní nádoby"
- [ 3] AO 241 367 o názvu "Vertikální fotogrammetrická souprava se světelnou rovinou"
- [ 4] Beneš B.: Počítačová grafika od 2D do 3D – 11. část, CHIP, ročník IX/1999, číslo 3, ISSN 1210-0684, 1999.
- [ 5] Černý I, Gavlovský E.: Odborná činnost na BMZ-referát na VIII svět. kongresu IMS v USA, IX.1991
- [ 6] Fojtů B., Dombrovský Z.: Coal Seam Extraction in Safety Shact Pillar, the Photogrammetric Measarament of a Shaft by the Veritikal Polygeometric traverse, září 1991, Kentucky USA
- [ 7] Kovář L: FOTCOUNT- Programátorská dokumentace, BMZ VŠB TU v Ostravě, 1992
- [ 8] Ličev L. - Holuša T.: Nové řešení důlní fotogrammetrie na PC, 2/1998, URGP Praha, 1998.
- [ 9] Ličev L.: New approaches to mining photogrammetry using PC, 5 nacionalna konferencija Varna '98, MGU Sofia, 1998.
- [10] Ličev, L.: Fotogrammetrie na PC, 4/1999, Acta montanistica slovac, Košice, SR, 1999.
- [11] Ličev L.: Fotogrammetrické měření důlních jam, 7/2001, URGP Praha, 2001.
- [12] Ličev L.: FOTOM 2000 a vizualizace procesu měření, Konference GIS '2001 VŠB-TU Ostrava, HGF, 2001.
- [13] Ličev L.: Podrobnější analýza snímků, 12. konference SDMG, Ostrava, VŠB HGF, 2005.
- [14] Ličev, L. - Holuša T.: Fotogrammetrické měření důlních jam, Konference GIS'99 VŠB TUO, HGF, 1999.
- [15] Ličev, L., Krahulec, L., Král, J.: Systém FOTOM 2009 na platformě NetBeans. In Proceedings - Symposium GIS Ostrava 2010. 2010 Hruha, Michal Podhorányi, VŠB TU Ostrava:VŠB TU Ostrava, 2010, čís. 1, Proceedings - Symposium GIS Ostrava 2010, p132-133, 8 str. VŠB TU Ostrava, ISBN 978-80-248-2171-9, 2010.
- [16] Pavelka K.: Fotogrammetrie 1/2009, 10/2003 a 20/2003, Vydavatelství ČVUT Praha
- [17] Serra, J.: Image Analysis and Matematical Morphology, Vol. 2, Academic Press, New York, 1988.
- [18] Sun Microsystems, Inc.: Modules API [online]. 2009 [citováno 2. Dubna 2009] Dostupné na: <<http://bits.netbeans.org/dev/javadoc/org-openide-modules/org-openide/modules/doc-files/api.html/>>
- [19] Sojka E.: Digitální zpracování obrazu, skriptá VŠB - TUO, FEECS, 1999.
- [20] Žára J. a kolektiv: Počítačová grafika – principy algoritmy, 1. vydání, GRADA, ISBN 80-85623-00-5, Praha, 1992.